

Determination of Wave Direction Using an Orbital Following Buoy

A.A. FERNANDES, A.M. ALMEIDA, R. VAITHIYANATHAN AND
P. VETHAMONY

National Institute of Oceanography, Dona Paula, Goa-403 004, India

ABSTRACT

Software has been developed in FORTRAN language using a personal computer for the determination of wave direction from time series measurements of heave, pitch and roll of an orbital following buoy. The method of digital band pass filtering described by Edward C. Brainard II of Endeco Inc. USA was used. A derivation of the basic formula used is presented. The software developed by us, viz. BUOY-D-PFOR, and the software provided by ENDECO, viz. 1156DBP. EXE, were both run for observed as well as computed simulated data. This is a preliminary report on program development. In the case of observed data, wave directions obtained with BUOY-D-P agreed within $\pm 5^\circ$ with the single available visual estimate of swell direction and within $\pm 50^\circ$ with directions obtained with 1156DBP. In the case of computer simulated data, BUOY-D-P was able to recover wave directions accurately for both mono-chromatic and multi-chromatic wave trains. 1156DBP was equally successful, except that if the simulated wave direction was θ , the computed direction was found to be $\pi + \theta$. This offset has been explained.

INTRODUCTION

For the determination of wave direction, two types of wave following buoys are used, viz. slope following buoys and orbital following buoys. In the case of a slope following buoy, the tilt of the buoy in the direction of the wave follows a simple harmonic motion having the frequency of the wave and is 90° out of phase with the wave motion (also with heave of the buoy) (Fig. 1a). Maximum tilt (positive and negative) is experienced on the slope of the wave at mean sea level. The buoy is level at the wave crest and trough. A slope following buoy has an inherent defect owing to its flat bottom "discus" shaped design. It is liable to capsize unless its diameter is larger (above 12 m). This type of buoy is also liable to give erroneous wave directions in the presence of breaking waves.

In the case of orbital following buoy, its tilt in the direction of the wave again follows a simple harmonic motion having the frequency of the wave

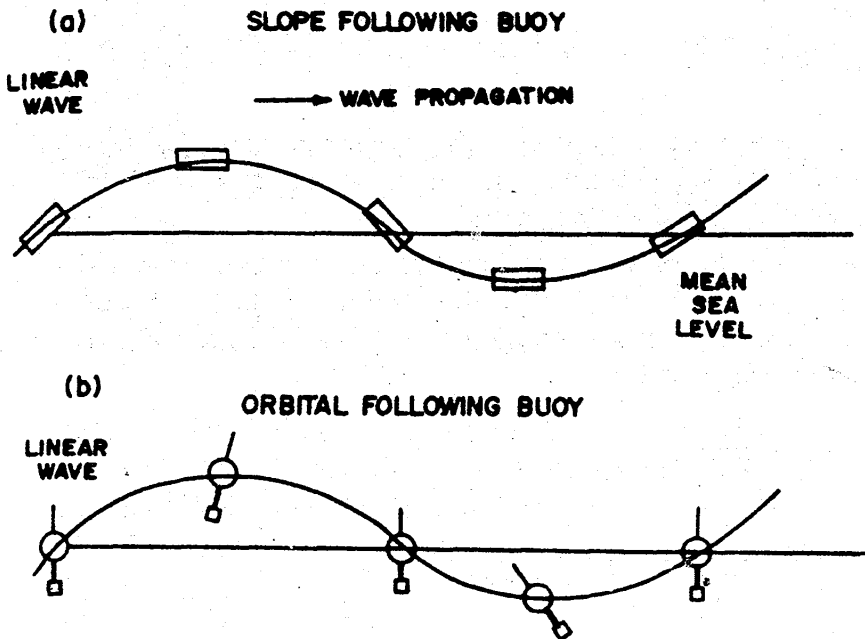


Fig. 1—Slope and orbital following buoy motions

but is in phase with the wave motion (also with heave of the buoy), (Fig. 1b). Maximum tilt (positive and negative) of the buoy occurs on the crest and trough of the wave. The buoy is level on the slope of the wave at mean sea level. This type of buoy is spherical in design, has a deeply suspended and rigidly attached ballast, behaves like an “inverted pendulum”, is inherently stable and cannot capsize. Also, breaking waves cannot introduce errors in the computation of wave direction.

Slope following buoys detect the vertical acceleration and the wave slope in the north-south and east-west directions. Tilt following buoys detect the vertical acceleration and the tilt of the buoy in the north-south and east-west direction. In both types of buoys, therefore, three independent measurements are made.

Slope following buoys came into existence first, and orbital following buoys came much later. The first slope following buoy was that of Longuet-Higgins, *et al.* [4] while perhaps the first orbital following buoy was that of Middleton, *et al.* [5]. The methodology created for the determination of the directional spectrum from the motions of a slope following buoy is being applied for orbital following buoys with slight modifications

METHODOLOGY

Theoretical basis

Consider a one-dimensional mono-chromatic linear wave

$$h(t) = \frac{H}{2} \cos(\kappa x - \sigma t) \quad \dots (1)$$

where h is the wave elevation with respect to time; H , the wave height; $\kappa (= 2\pi/L)$, the wave number; L , the wave length; $\sigma (= 2\pi/T)$, the angular frequency; and T , the wave period.

Let $z=0$ be the mean water line, the z -axis reckoned positive upwards, and d be the mean water depth. Then the horizontal component of orbital velocity, u , and the vertical component of fluid acceleration, α_z , due to the wave motion are given by:

$$u = \frac{\pi H \cosh[\kappa(z+d)]}{T \sinh(\kappa d)} \cos(\kappa x - \sigma t) \quad \dots (2)$$

$$\alpha_z = -\frac{g\pi H \sinh[\kappa(z+d)]}{L \cosh(\kappa d)} \cos(\kappa x - \sigma t) \quad \dots (3)$$

Ideally, an orbital following buoy simultaneously performs two motions: heave and tilt. Due to flotation, the buoy faithfully heaves up and down with the wave, i.e. it acts as a wave rider. And due to the horizontal component of orbital velocity, the buoy tilts positively and negatively in the direction of the wave, the tilt being proportional to the horizontal component of the orbital velocity, u . The tilt of the buoy is in phase with the wave elevation because of the presence of $+\cos(\kappa x - \sigma t)$ in Eqs (1) and (2).

As far as the tilt motion is concerned, the buoy acts as an inverted pendulum. This is achieved in practice by rigidly attaching to the buoy a deeply suspended ballast. The ballast acts as the fulcrum of the inverted pendulum, while the spherical buoy acts as the bob of the pendulum.

Due to the similarity between Eqs (1) and (3), the wave elevation is reckoned from the vertical acceleration of the buoy measured with an accelerometer. To determine the wave direction, besides the wave elevation, it is necessary to know the tilts of the buoy in the north-south and east-west directions. Two inclinometers measure the tilt in two mutually perpendicular directions with respect to a lubber's line on the buoy. These tilts, known as pitch and roll, are then converted into north-south and east-west tilts with the help of a two-axis flux gate compass. In the ENDECO system, the accelerometer, the two inclinometers and the two-axis flux gate compass are housed in the ballast of the buoy, while the electronics and the battery power supply are located in the spherical buoy.

Derivation of basic formula

We shall now present a derivation of the formula for the determination of wave direction from time series measurements of wave elevation (heave),

north-south tilt and east-west tilt of the buoy for a mono-chromatic wave. It is assumed that:

a) Let θ be the wave direction. The wave direction is the direction from which the wave front comes, and is reckoned clockwise positive with respect to the north axis.

$$b) \text{ Let } h(t) = H \cos \left(\frac{2\pi t}{T} + \delta \right)$$

where h is the wave elevation as a function of time t ; H , the amplitude of the wave; T , the period of the wave; and δ , the initial phase of the wave. Then the tilt of the buoy in the direction of the wave is given by

$$\phi(t) = \frac{cH}{T} \cos \left(\frac{2\pi t}{T} + \delta \right)$$

where c is a constant. A positive tilt indicates that the buoy is tilted towards the direction in which the wave front is going, while a negative tilt indicates that the buoy is tilted towards the direction from which the wave front is coming.

Case (i) [$\phi(t) < 0$]: In Fig. 2, θ is the wave direction; ϕ , the tilt of the buoy, and $P(x, y, z)$ is a point on the axis of the buoy. X-axis is along east, Y-axis along north and Z-axis vertically upwards. 0 is the lower extremity of the buoy; it is the point about which the buoy is tilting, i.e. the fulcrum. Note that since $\phi < 0$, the buoy is tilted towards the direction from which the wave front is coming. Then the north-south tilt, η , and the east-west tilt, ϵ , of the buoy are given by:

$$(N-S): \tan \eta = \frac{r \sin |\phi| \cos \theta}{r \cos |\phi|} = \frac{y}{z}$$

$$(E-W): \tan \epsilon = \frac{r \sin |\phi| \sin \theta}{r \cos |\phi|} = \frac{x}{z}$$

From the above two equations,

$$\theta = \tan^{-1} \left[\frac{\tan \epsilon}{\tan \eta} \right] \quad \dots (4)$$

By taking into consideration the signs of the numerator and denominator, θ is uniquely determined in the range $(0, 2\pi)$. In FORTRAN programming language, this is conveniently achieved by invoking the double argument function ATAN2 (Y,X).

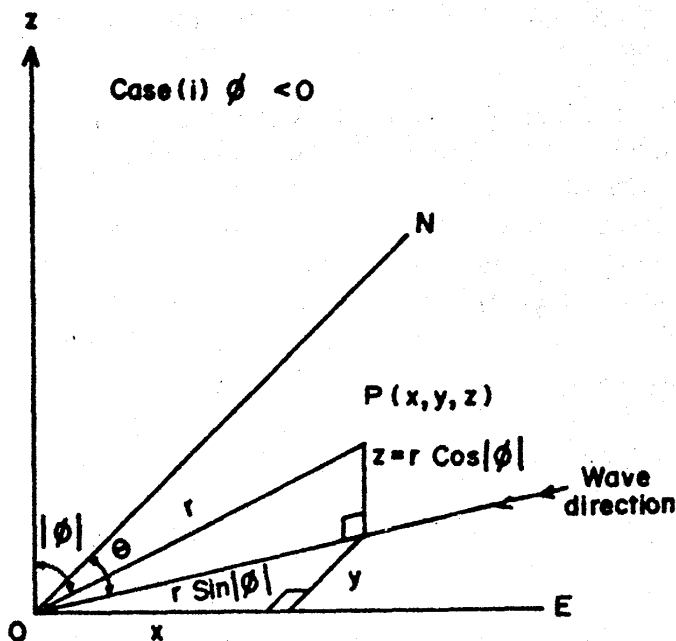


Fig. 2—Buoy tilts for wave troughs

Case (ii) [$\phi(t) > 0$]: This case is treated in Fig. 3. Note that since $\phi > 0$, the buoy is tilted towards the direction in which the wave front is going. In this case, the north-south tilt, η , and the east-west tilt, ϵ , are given by

$$\text{(N-S): } \tan \eta = \frac{r \sin \phi \cos(\theta + \pi)}{r \cos \phi} = \frac{y}{z}$$

$$\text{(E-W): } \tan \epsilon = \frac{r \sin \phi \sin(\theta + \pi)}{r \cos \phi} = \frac{x}{z}$$

And from the above two equations,

$$\theta = \tan^{-1} \left[\frac{-\tan \epsilon}{-\tan \eta} \right] \quad \dots (5)$$

By taking into consideration the signs of the numerator and denominator, θ is determined correctly and uniquely in the range $(0, 2\pi)$. It may be noted that since θ is determined in the range $(0, 2\pi)$ and not $(-\pi/2, \pi/2)$, Eqs (4) and (5), though similar, are two quite distinct formulae. It is also to be noted that Eq. (5), which is valid for all $\phi > 0$, is particularly valid for wave crests.

Brainard [1] has given the following formula for wave crests:

$$\theta = \tan^{-1}(\epsilon/\eta)$$

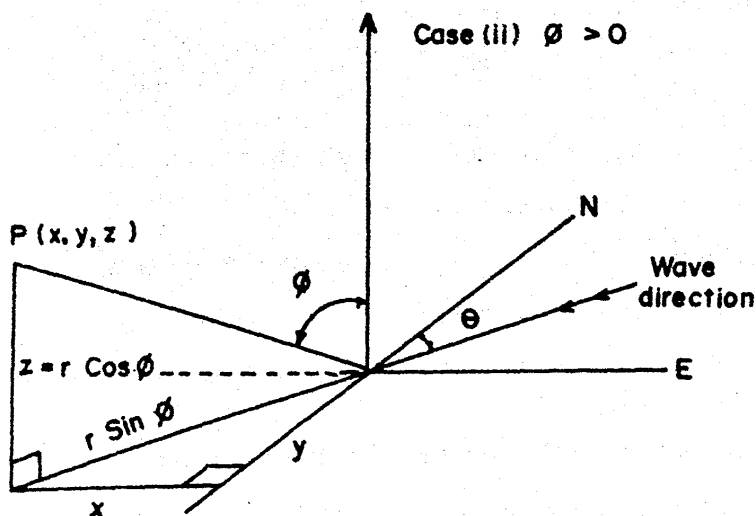


Fig. 3—Buoy tilts for wave crests

It may be noted that the above formula is an approximation of Eq. (5) that holds true for small values of η and ε , which generally is the case in practice. As we shall see later, the absence of the negative sign in the numerator and denominator is due to Brainard taking an inverted heave series as input for his computer program.

The software developed

Equations (4) and (5) are valid for monochromatic waves. The method of digital band-pass filtering assumes that these equations will be valid for high resolution spectral bands. Essentially, the method applies a band-pass filter to the heave, north-south tilt and east-west tilt series and uses Eq. (5) at each wave crest of the filtered series to determine the mean wave direction in the band.

Our software, viz. BUOY-D-P.FOR, runs in the manner indicated below. First, steps (1)-(3) are carried out. Then for each frequency band, steps (4)-(10) are performed. This is the main phase of the computations, as the mean wave direction and standard deviation of direction for each band are computed here. Lastly, in steps (11)-(13), the mean energy in each frequency band is computed and the essential results of the processing are printed.

- 1) Read heave, north-south tilt, and east-west tilt series, h , n , e respectively.
- 2) Perform FFT of h , n , e to obtain the Fourier transforms H , N , E respectively.
- 3) Save H , N , E in binary scratch files. Binary files are used for fast access.

- 4) *Read H, N, E.
- 5) *Band pass H, N, E, i.e. set the Fourier components outside the band to zero.
- 6) *Perform inverse FFT of H, N, E to obtain h, n, e.
- 7) *Determine the location of wave crests of h.
- 8) *Determine values of n and e corresponding to the wave crests.
- 9) *Determine the wave direction at each crest using Eq. (5).
- 10) *Determine the mean direction and standard deviation for the frequency band.
- 11) Use Blackman window on the original heave series.
- 12) Perform FFT of heave series.
- 13) Find mean energy in each band and scale the mean energy by a factor of $1/0.303$ to compensate for loss of energy due to windowing.

RESULTS AND DISCUSSION

Our software, viz. BUOY-D-PFOR, and the software provided by ENDECO, viz. 1156DBP.EXE, were both run for observed as well as computer simulated data. The observed data came from an ENDECO type 1156

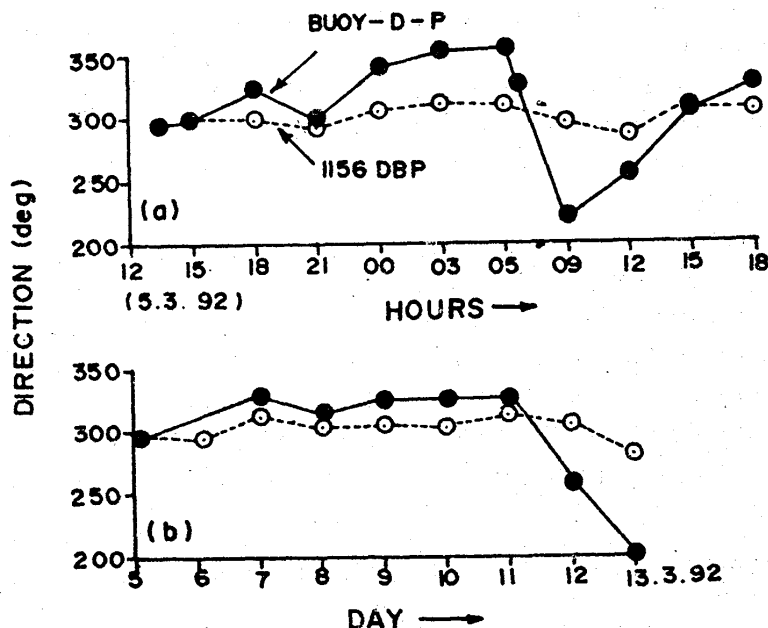


Fig. 4—Mean wave direction at peak frequency for a) 3 hourly records, and b) 24 hourly records

directional wave-track buoy system deployed for eight days off Candolim, Goa (lat. 15° 30'N; long. 73° 44'E) in a mean water depth of 14 m. Low wave conditions prevailed during the entire period. The significant wave height was in the range 0.53-0.96 m and the zero crossing period was in the range 4.36-5.99 sec. There were two main spectral peaks, one generally around 11.11 sec and the other around 5.56 sec, the latter peak being the more dominant nearly all the time.

In Fig. 4 are presented the mean directions at the peak frequency for two series of observed data: (i) 3 hourly records for one day from 1500 hrs

Table 1—Analysis of Observed Wave Data
[Date, 10 March 1992; No. of points, 2048; sampling interval, 0.5 sec]

Band No.	Centre Frequency (Hz)	Centre Per. (sec.)	Software BUOY-D-P			Software 1156DBP		
			Energy (m ² /Hz)	Dir. (deg)	Std. Dev. (deg)	Energy (m ² /Hz)	Dir. (deg)	Std. Dev. (deg)
1	0.03	33.33	0.06	325	003	0.10	350	012
2	0.04	25.00	0.08	321	002	0.11	001	008
3	0.05	20.00	0.03	325	002	0.03	262	007
4	0.06	16.67	0.01	324	001	0.02	252	009
5	0.07	14.29	0.06	324	002	0.05	320	005
6	0.08	12.50	0.05	323	002	0.09	242	009
7	0.09	11.11	0.09	324	001	0.07	273	006
8	0.10	10.00	0.05	324	001	0.03	267	008
9	0.11	9.09	0.02	325	001	0.01	249	005
10	0.12	8.33	0.01	324	002	0.01	194	008
11	0.13	7.69	0.01	324	001	0.01	278	004
12	0.14	7.14	0.02	325	001	0.02	309	005
13	0.15	6.67	0.02	324	001	0.02	311	002
14	0.16	6.25	0.13	323	001	0.10	308	002
15	0.17	5.88	0.07	324	001	0.14	307	001
16	0.18	5.56	0.14	325	001	0.16	303	001
17	0.19	5.26	0.19	325	002	0.14	302	001
18	0.20	5.00	0.15	326	001	0.09	302	001
19	0.21	4.76	0.06	324	003	0.07	308	001
20	0.22	4.55	0.04	323	002	0.07	310	001
21	0.23	4.35	0.05	324	002	0.04	305	002
22	0.24	4.17	0.07	324	002	0.10	300	001
23	0.25	4.00	0.09	323	002	0.10	308	001
24	0.26	3.85	0.02	324	003	0.04	302	001
25	0.27	3.70	0.07	324	002	0.07	308	001

on 5 March 1992, and (ii) 24 hourly records for 8 days from 1200 hrs on the same day. The figure shows that both the software show the same trends. The software 1156DBP shows more stable and perhaps more realistic wave directions. Directions computed by BUOY-D-P are within $\pm 50^\circ$ from those computed by 1156DBP.

At 1100 hrs on 10 March 1992, the swell direction was roughly estimated at 330° by visual observation. The results from two software for the record at 1200 hrs on the same day are presented in Table 1. It is seen that at the peak frequency (0.19 Hz), BUOY-D-P shows a mean wave direction of 325° , while 1156DBP shows the direction to be 302° . Both computed directions are close to the visual estimate. The data in Table 1 also show that the mean direction is more or less the same for all frequency bands in the case of BUOY-D-P. In the case of 1156DBP, wave directions show more scatter, specially at the low frequency end of the spectrum. This feature was noticed for all other records also.

The results obtained with the two software in the case of computer simulated data are discussed below. The characteristics of one record of simulated data which are similar to those of Fernandes *et al.* [2] are given in Table 2. In this record, essentially two wave trains were simulated. One wave train represented swell of approximately 11 sec coming from 000° . The other represented swell of around 6 sec coming from 120° . It is seen from Table 3 that BUOY-D-P computes the direction of both swells accurately. In the case of 1156DBP, we see that the mean direction of both swells is correct if we add $\pm 180^\circ$ to the computed direction. Additional computer runs showed the same feature. While BUOY-D-P reproduced wave directions correctly, 1156DBP directions showed an offset of 180° .

We found that this offset in the 1156DBP output could be removed by just reversing the signs of the simulated heave series. The presence of the

Table 2—Characteristics of Simulated Wave Data

[No. of sinusoids, 6; No. of points, 2048; sampling interval, 0.25 sec]

Wave train No.	AMP heave (m)	AMP tilt (deg)	Period (sec.)	Initial phase (deg)	Wave direction (deg)
1	0.1143	1.07	10.64	85	000
	0.1524	1.37	11.10	85	000
	0.1143	0.99	11.60	85	000
	0.1143	1.99	5.74	90	120
2	0.1524	2.59	5.88	90	120
	0.1143	1.90	6.01	90	120

Table 3—Analysis of Simulated Wave Data

[No. of points, 2048; sampling interval, 0.5 sec]

Band No.	Centre Freq. (Hz)	Centre Per. (sec.)	Software BUOY-D-P			Software 1156DBP		
			Energy (m ² /Hz)	Dir. (deg)	Std. Dev. (deg)	Energy (m ² /Hz)	Dir. (deg)	Std. Dev. (deg)
1	0.03	33.33	0.00	053	084	0.00	233	001
2	0.04	25.00	0.00	043	059	0.00	219	001
3	0.05	20.00	0.00	033	050	0.00	203	001
4	0.06	16.67	0.00	024	031	0.00	194	001
5	0.07	14.29	0.00	016	013	0.01	187	001
6	0.08	12.50	0.10	005	003	0.05	182	001
7	0.09	11.11	3.41	001	002	2.33	180	000
8	0.10	10.00	0.18	354	002	0.05	180	001
9	0.11	9.09	0.00	342	006	0.00	197	003
10	0.12	8.33	0.00	334	036	0.00	289	005
11	0.13	7.69	0.00	349	072	0.00	317	003
12	0.14	7.14	0.00	131	020	0.00	318	003
13	0.15	6.67	0.00	128	003	0.00	315	003
14	0.16	6.25	0.09	122	001	0.05	310	006
15	0.17	5.88	3.30	120	000	2.26	307	010
16	0.18	5.56	0.21	119	001	0.11	199	009
17	0.19	5.26	0.00	115	002	0.01	148	006
18	0.20	5.00	0.00	112	006	0.01	133	003
19	0.21	4.76	0.00	110	007	0.00	125	001
20	0.22	4.55	0.00	108	011	0.00	117	001
21	0.23	4.35	0.00	106	012	0.00	115	000
22	0.24	4.17	0.00	105	013	0.00	114	000
23	0.25	4.00	0.00	103	018	0.00	109	000
24	0.26	3.85	0.00	102	010	0.00	109	000
25	0.27	3.70	0.00	102	009	0.00	107	000

offset of 180° and the fact that 1156DBP uses Eq. (4) instead of Eq. (5) indicate that the heave series in the ENDECO observed data are actually inverted about the zero line. Thus, the observed offset is solely due to differing assumptions concerning the heave series.

Since in the case of simulated data there is an offset of 180° between directions computed by BUOY-D-P and 1156DBP, we cannot but conclude that the apparent consistency in the results in the case of observed data is by chance only. Application of empirically obtained frequency dependent

amplitude and phase corrections, as suggested by LeBlanc and Middleton [3] and incorporated in 1156DBP, might show the offset in the case of observed data also.

When we ran 1156DBP with computer simulated data using either a mono-chromatic train, or a multi-chromatic wave train whose component sinusoids were all from just one uniform direction, we observed an artifact of a backward travelling wave located in the higher frequencies. With BUOY-D-P, such an artifact was not present. The artifact of a backward travelling wave was observed by LeBlanc and Middleton [3].

For the record, we may mention that Brainard's paper [1] is unpublished. A CD-ROM computer search through the *Aquatic Sciences and Fisheries Abstracts (ASFA)* database did not list this particular article, though it listed several articles by the same author, including some apparently earlier work and some apparently later work.

CONCLUSION

Software has been developed indigenously for the determination of wave direction from time series measurements of heave, pitch and roll of an orbital following buoy. The software has been tested and validated with computer simulated data. Some modifications are needed for dealing with field data.

ACKNOWLEDGEMENT

The authors express their thanks to Mr. L.V.G. Rao for supporting this study, and to the Director, for the facilities provided. They are grateful to ENDECO (USA) for providing the format in which the ENDECO raw data is written, and to Mr. G. Navelkar for technical help.

REFERENCES

1. Brainard II, E.C. High resolution directional wave spectra using digital band pass filter method. (Included in ENDECO Manual).
2. Fernandes, A.A., A.D. Gouveia and R. Nagarajan. 1988. Determination of wave direction from linear and polygonal arrays. *Ocean Engg.*, 15(4): 345-357.
3. LeBlanc, L.R. and F.H. Middleton. 1982. Storm directional wave spectra measured with a single buoy. Oceans 82 Conference Record: Industry, Govt., Education-Partners in Progress-Washington D.C., 20-22 September 1982.
4. Longuet-Higgins, M.S., D.E. Cartwright and N.D. Smith. 1963. Observations of the directional spectrum of sea waves using the motion of a floating body. In: *Ocean Wave Spectra*. National Academy of Sciences: 111-136.
5. Middleton, F.H., L.R. LeBlanc and W.I. Sternberger. 1978. Wave direction measurement by a single wave follower buoy. Proc. 1978 Offshore Technology Conference, 8-10 May, Houston, Texas, No. OTC 3180.